





Thymosin β 4 promotes autophagy and repair via HIF-1 α stabilization in chronic granulomatous disease

Giorgia Renga^{1,*}, Vasilis Oikonomou^{1,*}, Silvia Moretti¹, Claudia Stincardini¹, Marina M Bellet¹, Marilena Pariano¹, Andrea Bartoli¹, Stefano Brancorsini¹, Paolo Mosci², Andrea Finocchi³, Paolo Rossi³, Claudio Costantini¹ , Enrico Garaci⁴, Allan L Goldstein⁵, Luigina Romani¹ 

Chronic granulomatous disease (CGD) is a genetic disorder of the NADPH oxidase characterized by increased susceptibility to infections and hyperinflammation associated with defective autophagy and increased inflammasome activation. Herein, we demonstrate that thymosin β 4 ($T\beta$ 4), a g-actin sequestering peptide with multiple and diverse intracellular and extracellular activities affecting inflammation, wound healing, fibrosis, and tissue regeneration, promoted in human and murine cells noncanonical autophagy, a form of autophagy associated with phagocytosis and limited inflammation via the death-associated protein kinase 1. We further show that the hypoxia inducible factor-1 (HIF-1) α was underexpressed in CGD but normalized by $T\beta$ 4 to promote autophagy and up-regulate genes involved in mucosal barrier protection. Accordingly, inflammation and granuloma formation were impaired and survival increased in CGD mice with colitis or aspergillosis upon $T\beta$ 4 treatment or HIF-1 α stabilization. Thus, the promotion of endogenous pathways of inflammation resolution through HIF-1 α stabilization is druggable in CGD by $T\beta$ 4.

DOI [10.26508/lsa.201900432](https://doi.org/10.26508/lsa.201900432) | Received 20 May 2019 | Revised 31 October 2019 | Accepted 4 November 2019 | Published online 12 November 2019

Introduction

Chronic granulomatous disease (CGD) is an immunodeficiency caused by mutations in the proteins forming the NADPH complex, which results in defective production of reactive oxygen species (ROS), impaired microbial killing by phagocytic cells, and increased susceptibility to infections (Rider et al, 2018). A common feature of CGD patients is the presence of a hyperinflammatory state in multiple organs, including the gastrointestinal and urogenital tract, lungs, and eyes (Rider et al, 2018), to which inflammation caused by

defective LC3-associated phagocytosis (LAP) greatly contributes (de Luca et al, 2014).

LC3-associated phagocytosis is a noncanonical autophagy pathway that plays a key role in the process of linking signals from phagocytosis to inflammation and innate immune responses (Henault et al, 2012; Martinez et al, 2016). Different from canonical autophagy, LAP is activated during phagocytosis upon recognition of microbes by pattern recognition receptors for rapid pathogen degradation (Simon & Clarke, 2016; Sprenkeler et al, 2016). The efficient clearance of the infectious products promoted by LAP could by itself be sufficient to reduce the inflammatory response and, hence, immunopathology. However, a mechanism by which inflammation is regulated during LAP has been recently described and involves the death-associated protein kinase 1 (DAPK1) (Oikonomou et al, 2016), a kinase mediating many different cellular functions such as cell death and repair (Bialik & Kimchi, 2006; Singh et al, 2016). Activated by IFN- γ , DAPK1 not only mediates LAP of the fungus *Aspergillus fumigatus* but also concomitantly inhibits nod-like receptor protein 3 (NLRP3) activation, thus restraining pathogenic inflammation (Oikonomou et al, 2016). Of interest, DAPK1 activity was defective in murine and human CGD (Oikonomou et al, 2016), a finding suggesting that the LAP/DAPK1 axis may represent a druggable pathway in CGD (Oikonomou et al, 2018).

Besides participating in direct microbial killing, the generation of ROS by the influx of neutrophils during infection is accompanied by local oxygen consumption that results in a condition known as inflammatory hypoxia, with stabilization of the hypoxia inducible factor-1 (HIF-1) α and resolution of inflammation (Campbell et al, 2014). This phenomenon is particularly relevant in the colonic mucosa, and the effect of HIF-1 α in the induction of angiogenesis- and glycolysis-related genes as well as genes involved in mucosal barrier protection has been validated in animal models of colitis and in human-derived colonic tissue (Campbell & Colgan, 2019). Consistent with the role of ROS in inflammatory hypoxia, most CGD

¹Department of Experimental Medicine, University of Perugia, Perugia, Italy ²Internal Medicine, Department of Veterinary Medicine, University of Perugia, Perugia, Italy ³Department of Pediatrics, Unit of Immune and Infectious Diseases, Children's Hospital Bambino Gesù, Rome, Italy ⁴University San Raffaele and Istituto di Ricovero e Cura a Carattere Scientifico San Raffaele, Rome, Italy ⁵Department of Biochemistry and Molecular Medicine, the George Washington University, School of Medicine and Health Sciences, Washington, DC, USA

Correspondence: luigina.romani@unipg.it

*Giorgia Renga and Vasilis Oikonomou contributed equally to this work

patients manifest inflammatory bowel disease-like symptoms (Campbell & Colgan, 2019), and pharmacological stabilization of HIF-1 α within the mucosa protected CGD mice from severe colitis (Campbell et al, 2014). Although the contribution of inflammatory hypoxia in the lung is disputed (Taylor & Colgan, 2017), hypoxia develops during pulmonary invasive fungal infection in models of invasive aspergillosis, including CGD mice (Grahl et al, 2011), and HIF-1 α stabilization is required for protection (Shepardson et al, 2014). Of note, HIF-1 α mediates the autophagic process induced by a hypoxic environment (Bellot et al, 2009), thus raising the interesting hypothesis that a defective HIF-1 α induction/stabilization in CGD patients might be causally related to the impaired autophagy and that pharmacological stabilization of HIF-1 α might restore LAP/DAPK1 and immune homeostasis during infection with CGD.

Thymosin β 4 (T β 4) is a major g-actin sequestering peptide found in eukaryotic cells and represents 70–80% of the total thymosin content in human tissues. It is an active peptide with 43 amino acids with moonlighting properties and multiple and diverse intracellular and extracellular activities (Goldstein et al, 2005). Several physiological properties of T β 4 have been reported, including the regulation of wound healing, inflammation, fibrosis, and tissue regeneration (Goldstein et al, 2012). The circumstantial evidence points to T β 4 as a potential molecule that could link HIF-1 α stabilization to LAP in CGD. First, T β 4 promotes HIF-1 α stabilization (Oh et al, 2008; Jo et al, 2010; Oh & Moon, 2010) and, in turn, HIF-1 α may transcriptionally regulate T β 4 expression (Ryu et al, 2014). Second, T β 4 is the major actin-sequestering molecule in all eukaryotic cells (Ballweber et al, 2002) and the actin networks contribute to autophagosome formation and membrane remodeling during autophagy (Aguilera et al, 2012), which suggests a possible role for T β 4 in autophagy.

Based on these premises, in the present study, we have resorted to in vitro and in vivo studies involving human cells and mice with CGD to provide evidence that T β 4 promotes LAP involving DAPK1 in murine and human CGD although concomitantly impairing granuloma formation in the lung and gut of mice with CGD. Both autophagy and repair were dependent on HIF-1 α stabilization, in the lung and likely in the gut, a finding qualifying T β 4 as a promising peptide with beneficial effects in CGD through the promotion of endogenous pathways of autophagy and inflammation resolution.

Results

T β 4 promotes LC3-associated phagocytosis involving DAPK1

In order to assess the ability of T β 4 to promote autophagy, we first evaluated the ratio of LC3-II to LC3-I, widely used to monitor autophagy (Oikonomou et al, 2016), on RAW264.7 cells exposed to live *Aspergillus* conidia in the presence of different concentrations of T β 4. We have already shown that internalized conidia undergo swelling and concomitantly induce autophagy in these cells (de Luca et al, 2014; Oikonomou et al, 2016). Immunoblotting revealed that T β 4, although not inducing autophagy in unpulsed cells (Fig 1A), dose-dependently increased the LC3-II to LC3-I ratio in cells pulsed with conidia, an effect observed as early as 2 h after the exposure to the fungus (Fig 1B). This finding suggests that T β 4 could

be able to activate LAP. To confirm this, the expression of DAPK1 and Rubicon proteins, known to be involved in LAP (Martinez et al, 2016), was dose-dependently increased by T β 4 (Fig 1C), a finding suggesting that T β 4 promotes noncanonical autophagy involving DAPK1 and Rubicon. This result prompted us to assess the ability of T β 4 to restore LAP in CGD, in vitro and in vivo. To this purpose, we purified macrophages from the lungs of C57BL/6 and *p47^{phox}-/-* mice and pulsed them in vitro with *A. fumigatus* conidia in the presence of T β 4. Consistent with previous findings (de Luca et al, 2014; Oikonomou et al, 2016), both autophagy and DAPK1 expression were defective in the cells from *p47^{phox}-/-* mice but were dose-dependently restored by T β 4 (Fig 1D). Confirming the murine observation, T β 4 also increased LC3B expression in monocytes from CGD patients exposed to *Aspergillus* conidia in vitro (Fig 1E), a finding suggesting that T β 4 is able to restore LAP involving DAPK1 in human CGD. For in vivo, we resorted to two different experimental models that mimic the human pathology, such as lung and gut inflammation. To this purpose, we infected C57BL/6 and *p47^{phox}-/-* mice with *A. fumigatus* intranasally and treated them with T β 4 for 7 consecutive days starting a week after the infection. LC3-II (Fig 1F) and DAPK1 (Fig 1G) expression were both defective in *p47^{phox}-/-* mice but restored by T β 4 and ablated (LC3-II) upon siT β 4 (Fig S1). For gut inflammation, we resorted to the acute colitis in *p47^{phox}-/-* mice by administering 2.5% dextran sulfate sodium (DSS) in drinking water for 7 d followed by 7 d of DSS-free autoclaved water. T β 4 was therapeutically administered daily for 7 d, after DSS treatment, at the time at which mice started to lose weight. The DSS treatment has been reported to repress *Dapk1* gene expression in colonic epithelial cells (Takeshima et al, 2012). Consistent with previous findings (de Luca et al, 2014), LC3-II (Fig 1H) and DAPK1 (Fig 1I) expression were both defective in the colon of *p47^{phox}-/-* mice with colitis as opposed to WT mice but restored upon treatment with T β 4 (Fig 1H and I).

T β 4 promotes HIF-1 α expression in CGD

Given that the defective LAP in CGD is amenable to restoration by T β 4, we wonder whether the production of T β 4 could be defective in CGD. To this purpose, we assessed T β 4 gene and protein expression in *p47^{phox}-/-* mice. We found a lower expression of T β 4 in CGD lungs than that in C57BL/6 mice, both in terms of gene and protein expression, as revealed by real-time (RT) PCR and immunoblotting (Fig 2A) and confirmed by immunofluorescence staining (Fig 2B). Given the reciprocal regulation between T β 4 and HIF-1 α (Oh et al, 2008; Ryu et al, 2014), we assessed whether defective T β 4 levels in CGD mice could be associated with altered HIF-1 α expression. This turned out to be the case, as HIF-1 α levels were reduced in CGD mice (Fig 2C and D) and T β 4 ablation decreased HIF-1 α in C57BL/6 mice (Fig S1A). Interestingly, administration of T β 4 could restore HIF-1 α levels in CGD mice (Fig 2E and F), whereas HIF-1 α silencing decreased T β 4 expression (Fig 2B). Defective T β 4 expression (Fig 2G) and restoration of HIF-1 α expression upon administration of T β 4 (Fig 2H) were also observed in the colon. Consistent with the murine results, T β 4 also increased HIF-1 α expression in monocytes from CGD patients challenged with *Aspergillus* conidia (Fig 2I), thus suggesting that T β 4 is able to restore HIF-1 α expression in human CGD. These results indicate that intracellular autocrine crosstalk between T β 4 expression and HIF-1 α induction occurs in CGD.

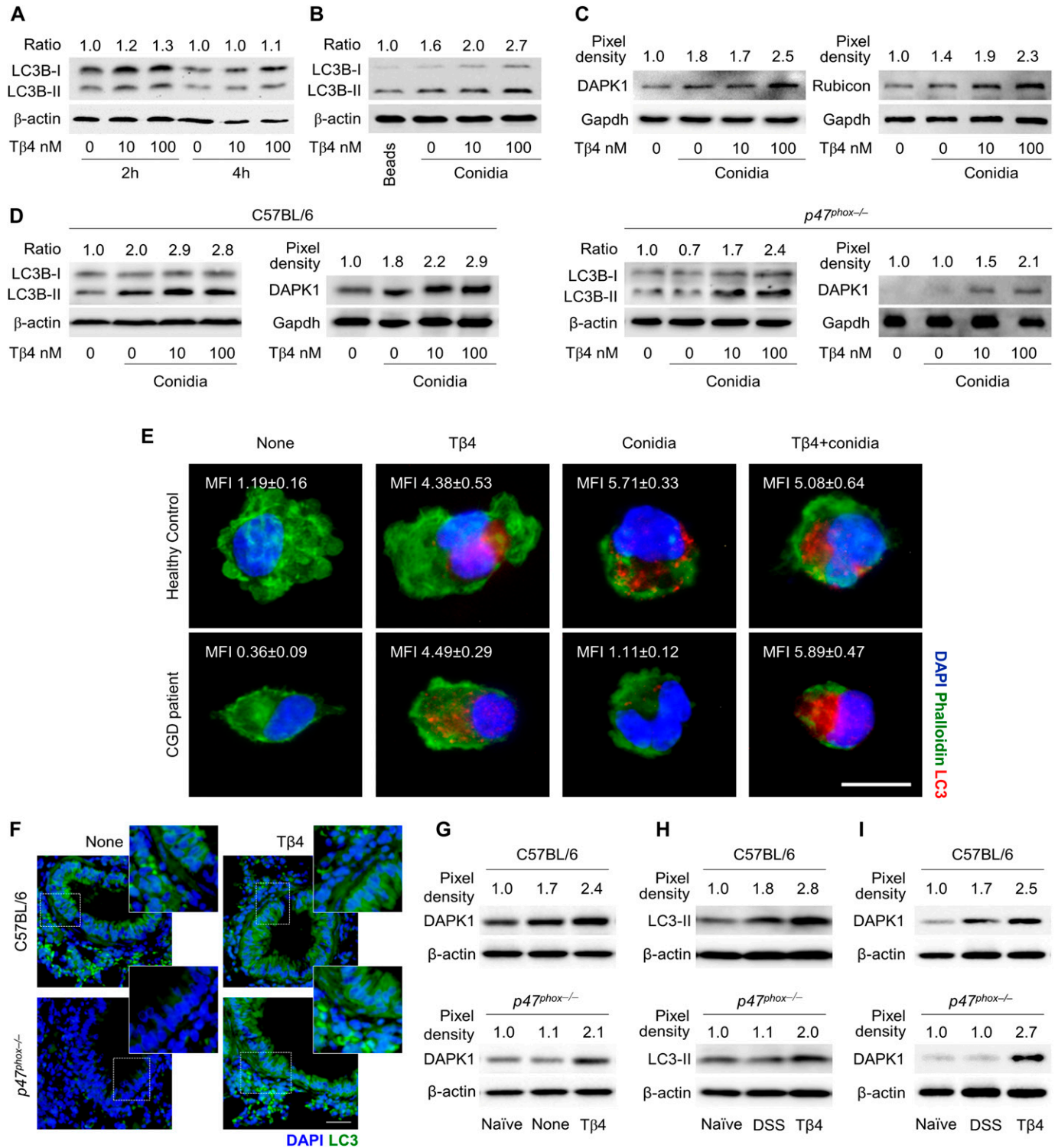


Figure 1. Tβ4 promotes LC3-associated phagocytosis involving DAPK1.

(A) LC3B-II/LC3B-I expression in RAW264.7 cells after 2 or 4 h stimulation with 10 and 100 nM Tβ4. (B, C) LC3B-II/LC3B-I and (C) DAPK1 and Rubicon expression in RAW264.7 cells pulsed for 2 h with *A. fumigatus* conidia after 1-h pretreatment with 10 and 100 nM of Tβ4. In (B), inert beads were used as the control. (D) LC3B-II/LC3B-I and DAPK1 production in lung macrophages from C57BL/6 and *p47^{phox}-/-* mice after pulsing with *A. fumigatus* conidia in the presence of Tβ4. (E) LC3 expression on monocytes from CGD patients or healthy controls pretreated with 100 nM Tβ4 and stimulated for 2 h with the fungus. (F, G) LC3 and (G) DAPK1 expression on the lung of C57BL/6 and *p47^{phox}-/-* mice infected intranasally with *A. fumigatus* conidia and treated i.p. with 5 mg/kg Tβ4 for 7 consecutive days starting a week after the infection. (H, I) LC3 and (I) DAPK1 expression in colon lysates of C57BL/6 and *p47^{phox}-/-* mice subjected to DSS-induced colitis for a week and treated i.p. with 5 mg/kg Tβ4 for 7 consecutive days after DSS treatment. Normalization was performed on mouse β-actin or Gapdh and corresponding pixel density is depicted. LC3-II band density was normalized to LC3-I to

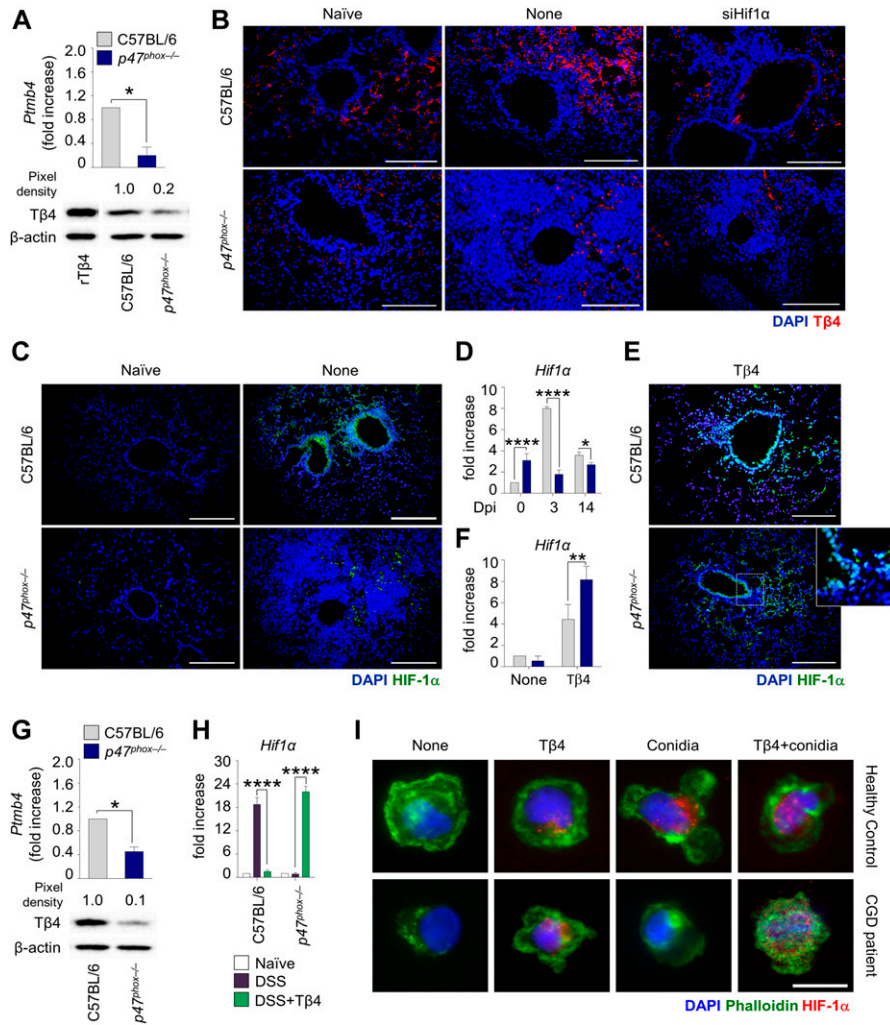


Figure 2. Tβ4 promotes HIF-1α expression in CGD. (A, B) Tβ4 gene expression (*Ptmb4*) and protein levels in the lung of uninfected mice and (B) Tβ4 expression in C57BL/6 and *p47^{phox-/-}* mice infected intranasally with the fungus and treated with Tβ4. (C, D) HIF-1α expression in the lung of infected mice. (E, F) HIF-1α expression in the lung of C57BL/6 and *p47^{phox-/-}* mice infected and treated with Tβ4. Mice were euthanized 7 d after infection. (G, H) Tβ4 gene expression (*Ptmb4*) and protein levels, and (H) HIF-1α gene expression in the colon of mice subjected to DSS-induced colitis for a week and treated i.p. with 5 mg/kg Tβ4 for 7 consecutive days after DSS treatment. (I) HIF-1α expression on monocytes from CGD patients or healthy controls pretreated with Tβ4 and stimulated for 2 h with the fungus. Gene expression was performed by real-time (RT)-PCR. For immunoblotting, normalization was performed on mouse β-actin, and corresponding pixel density is depicted. Recombinant (r)Tβ4 was used as a positive control. For immunofluorescence, nuclei were counterstained with DAPI. HIF-1α mean fluorescence intensity was measured with ImageJ software. Photographs were taken with a high-resolution microscope (Olympus BX51), 40×, and 100× magnification. For immunofluorescence, data are representative of two independent experiments. For RT-PCR, data are presented as mean ± SD of at least two independent experiments. Each independent in vivo experiment includes 6–8 mice per group. **P* < 0.05, *****P* < 0.0001, *p47^{phox-/-}* versus C57BL/6, Tβ4-treated versus untreated (DSS) mice. Unpaired t test or two-way ANOVA, Bonferroni post hoc test. Dpi, days post infection; Naive, uninfected mice. None, control siRNA-treated mice or untreated cells.

Tβ4 promotes LAP and mucosal barrier protection in an HIF-1α-dependent manner

To assess whether a causal link exists between HIF-1α stabilization and induction of autophagy by Tβ4, we first observed that Tβ4 induced the expression in vitro of *Bnip3* and *Bnip3l*, known to be involved in hypoxia-induced autophagy (Bellot et al, 2009) (Fig S2A). To assess this in vivo, we infected *p47^{phox-/-}* mice with *A. fumigatus* intranasally and treated them with Tβ4 in the presence or absence of siRNA for HIF-1α. The restoration of LC3-II (Fig S2B) expression in *p47^{phox-/-}* mice by Tβ4 was abrogated by HIF-1α inhibition, thus indicating that Tβ4 requires HIF-1α to induce LAP. Moreover, as HIF-1α is also directly involved in mucosal barrier protection in hypoxia (Campbell & Colgan, 2019), this would predict a role for Tβ4 in mucosal protection. To prove this, we selected genes known to be regulated by HIF-1α and measured their levels in vivo after treatment with Tβ4. Our screening revealed that

genes involved in angiogenic signaling (*Angpt2*, *Tie2*, and *Vegfa*), remodeling (*Fgf2*), hormonal regulation (*Epo*), and cell migration (*Cxcr4*) were all up-regulated in the lungs of *Aspergillus*-infected mice upon treatment with Tβ4 (Fig S2C). A similar up-regulation occurred in colons of *p47^{phox-/-}* mice in the DSS-induced colitis model (Fig S2D). Strikingly, treatment with HIF-1α siRNA completely abrogated the up-regulation induced by Tβ4 in the lung (Fig S2C). Overall, our results indicate that HIF-1α mediates fundamental effects of Tβ4, in the lung and likely in the gut, including LAP and induction of genes involved in the angiogenesis and repair, thus pointing to the Tβ4-HIF-1α axis as a potential therapeutic pathway in CGD.

Tβ4 ameliorates tissue and immune pathologies in CGD mice

These results would anticipate a beneficial effect of Tβ4 in diseased CGD mice. To this purpose, we evaluated the effect of Tβ4 in mice

obtain the ratio. For immunofluorescence, nuclei were counterstained with DAPI. Photographs were taken with a high-resolution microscope (Olympus BX51), 40×, and 100× magnification. LC3 mean fluorescence intensity was measured with ImageJ software. Data are representative of two independent experiments. Each independent in vivo experiment includes 6–8 mice per group. Data are presented as mean ± SD. Naive, uninfected, or untreated mice; None, infected mice.

with aspergillosis and colitis. The $p47^{phox-/-}$ mice are known to be highly susceptible to pulmonary aspergillosis and inflammation (Romani et al, 2008). Mice were monitored for fungal growth, antifungal activity of effector cells, survival, lung histopathology, and innate and adaptive Th immunity. Thymosin $\beta 4$ reduced the fungal growth in the lung of both types of mice (Fig 3A), an effect to which the ability of $T\beta 4$ to potentiate phagocytosis and fungal killing of effector phagocytes likely contributed (Fig 3B), and significantly increased the survival of infected mice, being more than 50% of mice survived at the time of which all the untreated mice have died (Fig 3C). Impressively, in $p47^{phox-/-}$ mice, gross lung pathology and histological examination (Fig 3D) revealed no signs of inflammatory lung injury and granuloma formation after $T\beta 4$ administration. Conversely, $T\beta 4$ deficiency by means of si $T\beta 4$ administration promoted lung pathology in C57BL/6 mice (Fig S1B). Consistent with the finding that resistance to infection could be restored in these mice by dampening inflammation through NLRP3/IL-1 β blocking (de Luca et al, 2014; Iannitti et al, 2016), $T\beta 4$ down-regulated NLRP3 expression in these mice (Fig 3E) and, accordingly, reduced IL-1 β , along with TNF- α , IL-17A, and increased IFN- γ production, an effect negated upon siHif1 α treatment (Fig 3F). Pathogenic Th2/Th17/Th9 cell responses were down-regulated and protective Th1/Treg cell responses promoted upon $T\beta 4$ treatment (data not shown). Strikingly, the effects on tissue pathology (Fig 3D) and inflammatory expression (Fig 3E) were all abolished by treatment with HIF-1 α siRNA, further strengthening the relevance of HIF-1 α in mediating $T\beta 4$ effects. These results suggest that $T\beta 4$ ameliorates inflammation and granuloma formation in the CGD lung via HIF-1 α . In the murine colitis model, mice were evaluated a day after $T\beta 4$ treatment for weight loss, colon histology, cytokine levels, and tight junction gene expression. Consistent with previous findings (de Luca et al, 2014; Falcone et al, 2016), $p47^{phox-/-}$ mice lost more weight than C57BL/6 mice (about 50% loss of their initial body weight on day 14) (Fig 4A) and had more severe colitis as observed by significantly increased disease activity index scores (Fig 4B). Hematoxylin and eosin staining of colon sections showed severe patchy inflammation characterized by transmural lymphocytic infiltrates, epithelial ulceration, and complete crypt loss (Fig 4C). In addition, $p47^{phox-/-}$ mice displayed high levels of NLRP3 expression (Fig 4D) and IL-1 β production (Fig 4E), along with high levels of myeloperoxidase (MPO), TNF- α , and IL-17A (Fig 4F) and low levels of TGF- β (Fig 4G). Treatment with $T\beta 4$ significantly led to weight regain (Fig 4A), decreased disease activity index scores (Fig 4B), amelioration of inflammatory pathology and tissue architecture (Fig 4C), decreased NLRP3 expression (Fig 4D) and inflammatory cytokine levels (Fig 4E and F), and up-regulation of the anti-inflammatory cytokines (Fig 4G). Of interest, $T\beta 4$ greatly promoted the expression of both *Cldn1* and *Ocln*, tight junction proteins that regulate intestinal permeability (Gunzel & Yu, 2013; Kyoko et al, 2014) (Fig 4H), thus suggesting a positive effect on the mucosal barrier function. The protective effect of $T\beta 4$ also occurred when treatment was given concomitantly with DSS (that is, from day 0 to day 7 [Fig S3]), a finding suggesting that prophylactic $T\beta 4$ is also beneficial. Altogether, these results suggest that $T\beta 4$, by activating LAP-DAPK1 and inhibiting inflammasome activity, could have beneficial effects on the outcome of colitis in CGD.

HIF-1 α stabilization recapitulates the effects of $T\beta 4$

Because HIF-1 α mediates the effects of $T\beta 4$ in CGD, we sought to investigate whether the stabilization of HIF-1 α independent of $T\beta 4$ could similarly exert beneficial effects. For this reason, given the well-known beneficial effects of HIF-1 α stabilization on disease outcomes and barrier function in animal models of intestinal inflammation (Colgan et al, 2015), we treated $p47^{phox-/-}$ mice with aspergillosis with dimethylxalylglycine (DMOG)—a cell-permeable competitive inhibitor of prolyl hydroxylase (PHD) that stabilizes HIF-1 α (Mole et al, 2003)—for 5 d. Similar to $T\beta 4$, DMOG reduced fungal burden (Fig 5A), ameliorated lung pathology (Fig 5B), increased HIF-1 α expression (Fig 5C), and up-regulated HIF-1 α -responsive genes (Fig 5D). Thus, HIF-1 α stabilization could be a therapeutic target in CGD.

Discussion

The results of the present study show that $T\beta 4$ restored autophagy and up-regulated hypoxia-responsive genes in human and murine CGD and this resulted in amelioration of disease pathology (Fig 5E). The increased autophagy, epithelial barrier protection, and repair induced by $T\beta 4$ are consistent with its antioxidative and anti-apoptotic effects (Kumar & Gupta, 2011) and represents a plausible mechanism through which inflammation and granuloma formation are balanced in CGD by $T\beta 4$. It is clear that the innate immune system is pivotal in orchestrating granuloma formation in response to microbial and foreign body challenge (Petersen & Smith, 2013). Impaired antibacterial autophagy links inflammation to granuloma formation in intestinal diseases (Lassen & Xavier, 2018). By promoting LAP, $T\beta 4$ may successfully contribute to pathogen elimination, thus clearly preventing granuloma formation. Thus, the beneficial activity of $T\beta 4$ may encompass a possible activity on the microbial composition at different body sites. Moreover, by inducing TGF- β (Sosne et al, 2004)—known to modulate the fibrotic repair process accompanying granuloma healing (Limper et al, 1994)— $T\beta 4$ may impair granuloma formation. However, excess TGF- β activity, by preventing effective granuloma formation, may interfere with antimicrobial mechanisms (Toossi et al, 1995). Thus, whether the high levels of TGF- β (Toossi et al, 1995) and $T\beta 4$ (Kang et al, 2014) observed in granulomatous lung lesions or colorectal cancer (Gemoll et al, 2015) are the cause or effect of defective granuloma formation needs clarification.

In lung aspergillosis, and likely in DSS-induced colitis, the effects of $T\beta 4$ were dependent on HIF-1 α that mediated not only the induction of autophagy but also the up-regulation of hypoxia-responsive genes. Interestingly, $T\beta 4$ up-regulated HIF-1 α -dependent genes, involved in barrier protection and angiogenesis and not in glycolysis, are known to contribute to inflammation in myeloid cells (Palazon et al, 2014) (Fig S4A), thus suggesting the unique ability of $T\beta 4$ to activate physiologic HIF-1 α to resolve inflammation. HIF-1 α can be regulated by both oxygen-dependent and oxygen-independent mechanisms in hypoxic and normoxic conditions, respectively, and strategies are being studied to either activate or inhibit the activity of HIF-1 α depending on the clinical setting (Giaccia et al, 2003; Yee Koh et al, 2008). Indeed, whereas HIF-1 α inhibition is recognized as an antitumor

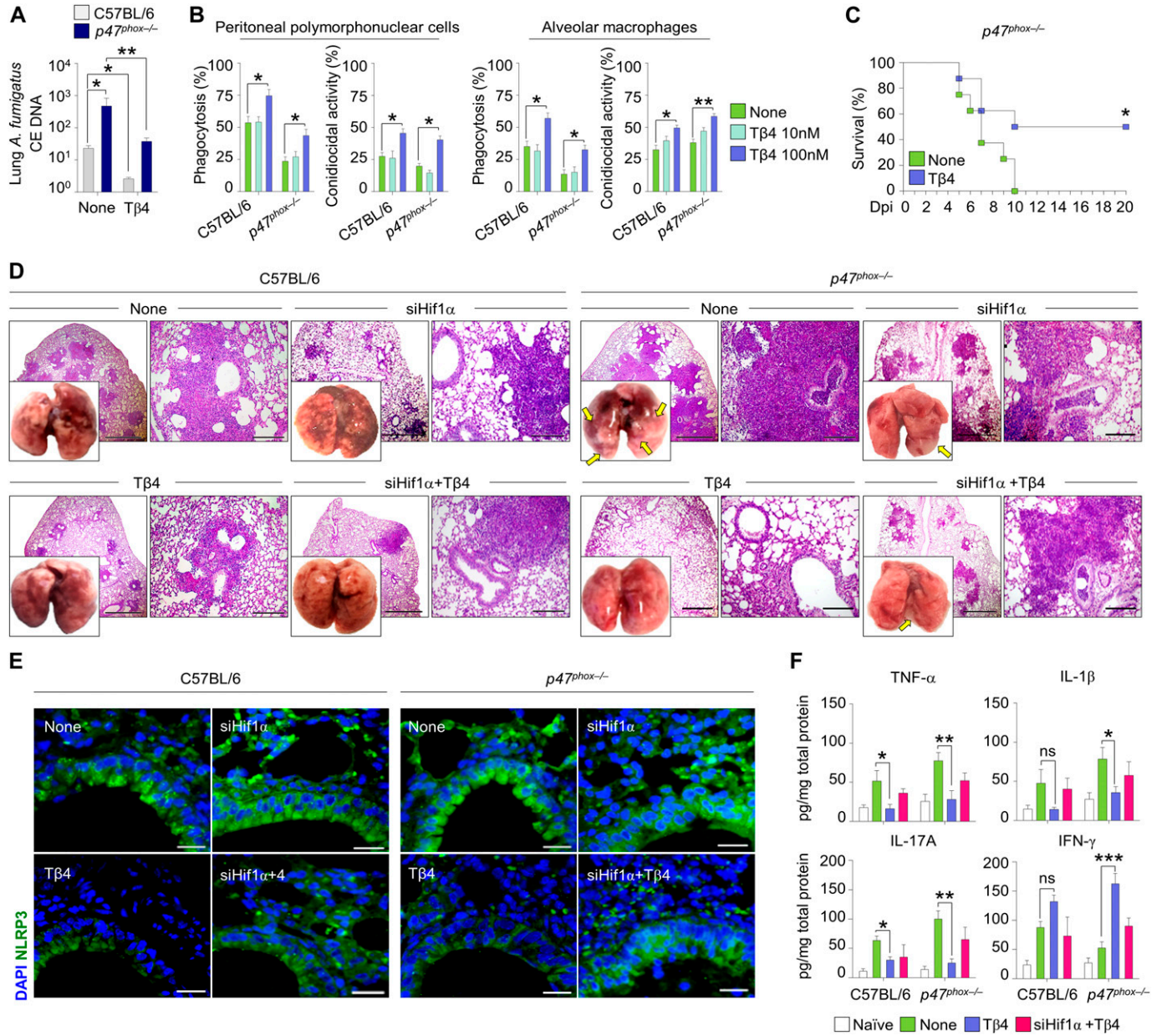


Figure 3. Tβ4 ameliorates tissue and immune pathologies in CGD mice.

(A) Lung fungal growth of C57BL/6 and *p47^{phox-/-}* mice infected intranasally with *A. fumigatus* conidia and treated i.p. with 5 mg/kg Tβ4 for 7 consecutive days starting a week after the infection. (B) Percent of phagocytosis and conidiocidal activity on peritoneal PMN cells and alveolar macrophages from uninfected C57BL/6 and *p47^{phox-/-}* mice pre-exposed to different doses of Tβ4 for 1 h before 2 h of pulsing with live *Aspergillus* conidia. (C) Survival curves for *p47^{phox-/-}* mice infected intranasally with *A. fumigatus* conidia and treated for 5 d with Tβ4. (D, E, F) Lung gross pathology and histology (periodic acid-Schiff [PAS] staining), (E) NLRP3 expression and (F) cytokines production on lung homogenates of infected mice treated with Tβ4 or siHif1α. For immunofluorescence, nuclei were counterstained with DAPI. Photographs were taken with a high-resolution microscope (Olympus BX51), 4×, 20×, and 40× magnification. Secreted cytokines were assayed by ELISA from supernatants. For histology and immunofluorescence, data are representative of two independent experiments. For RT PCR and ELISA, data are presented as mean ± SD of at least two independent experiments. Each independent in vivo experiment includes 6–8 mice per group. **P* < 0.05, ***P* < 0.01, ****P* < 0.001, *p47^{phox-/-}* versus C57BL/6 mice, Tβ4-treated versus untreated (None) mice or cells. Statistical analyses of the survival curves were performed using the log-rank (Mantel–Cox) test. Two-way ANOVA, Bonferroni post hoc test. Dpi, days post infection; None, control siRNA-treated mice; Naive, uninfected mice; ns, not significant.

therapeutic strategy, up-regulation of HIF-1α is critical in the treatment of ischemic states (Giaccia et al, 2003; Yee Koh et al, 2008). In the context of CGD, HIF-1α was underexpressed in the gastrointestinal mucosa and lung, suggesting that a potential therapy for CGD should include the elevation of HIF-1α levels to restore the

hypoxia-mediated tissue homeostasis and the optimal antimicrobial response. It has indeed been reported that hypoxia and HIF proteins are required for protection against *Pseudomonas aeruginosa* in vitro (Schaible et al, 2013) and against *A. fumigatus* in vivo (Shepardson et al, 2014).

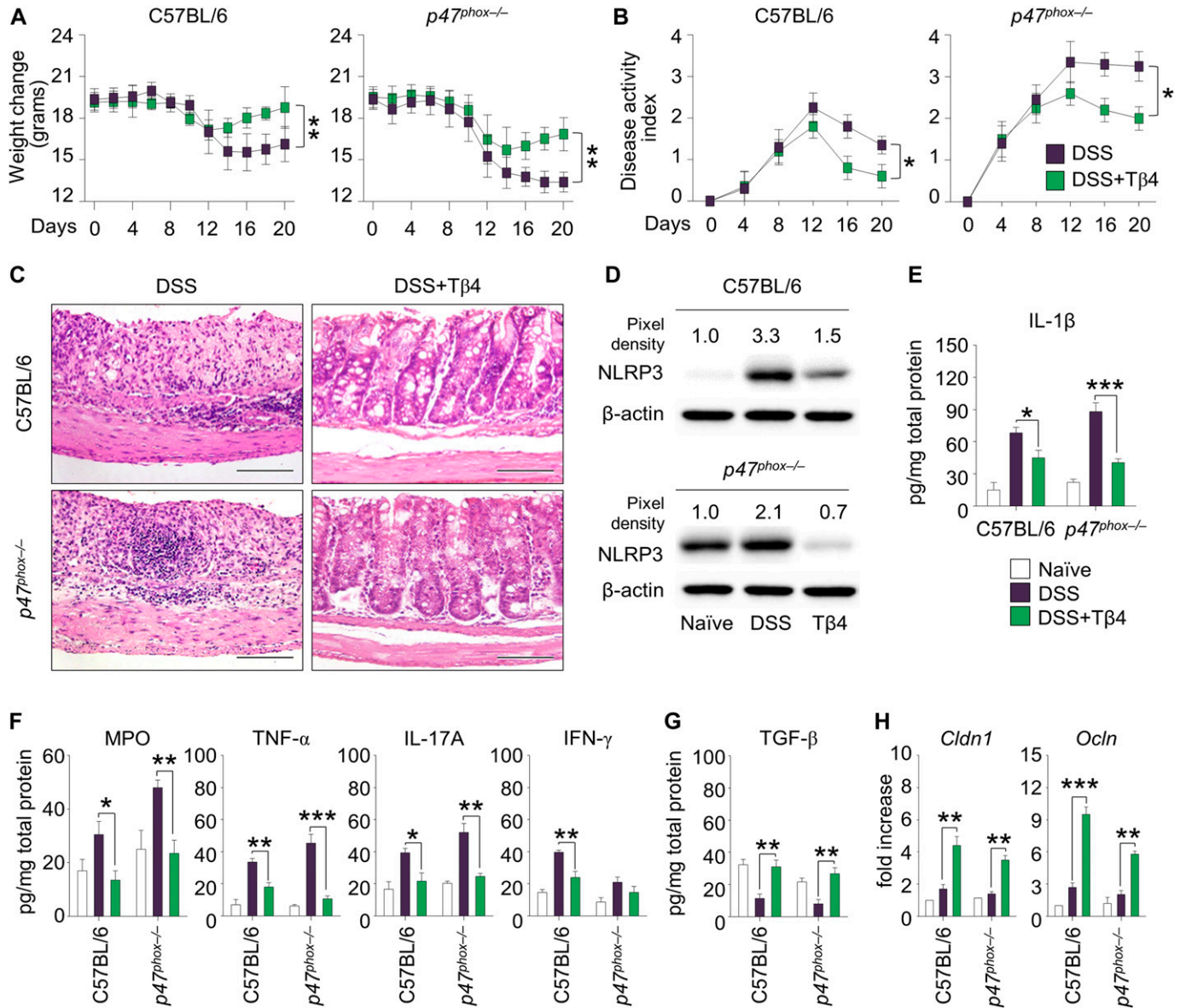


Figure 4. Tβ4 protects mice with CGD from DSS-induced colitis.

C57BL/6 and *p47^{phox-/-}* mice were subjected to DSS-induced colitis for a week and treated i.p. with 5 mg/kg Tβ4 for 7 consecutive days after DSS treatment. (A, B, C, D, E, G, H) A day after Tβ4 treatment, mice were evaluated for (A) weight change, (B) clinical disease activity index, (C) histological assessment of colitis severity (hematoxylin and eosin staining), (D) NLRP3 protein expression in colon, (E, F) levels of proinflammatory cytokines in colon homogenates, (G) TGF-β production, and (H) *Cldn1* and *Ocln* expression in the colon. Secreted cytokines were assayed by using ELISA from supernatants. Gene expression was performed by RT PCR. For immunoblotting, normalization was performed on mouse β-actin, and corresponding pixel density is depicted. Images were taken with a high-resolution microscope (Olympus BX51), 40× magnification. For histology and immunoblotting, data are representative of two independent experiments. For RT PCR and ELISA, data are presented as mean ± SD of at least two independent experiments. Each independent in vivo experiment includes 10 mice per group. **P* < 0.05, ***P* < 0.01, ****P* < 0.001, Tβ4-treated versus untreated (DSS) mice. Two-way ANOVA, Bonferroni or Tukey post hoc test. Naïve, untreated mice.

The dependency of Tβ4 activity on HIF-1α in lung aspergillosis, and likely in DSS-induced colitis, underpins a more general relationship between the two molecules. In agreement with the published literature (Oh et al, 2008; Ryu et al, 2014), we found that Tβ4 and HIF-1α crossregulate their reciprocal expression being the levels of HIF-1α defective in CGD mice but restored by Tβ4 and, conversely, silencing of HIF-1α in wild-type mice being associated with reduced levels of Tβ4. Several mechanisms might underlie the ability of Tβ4 to regulate HIF-1α expression. Thymosin β4 may inhibit PHDs that target

HIF-1α to degradation. Prolyl hydroxylases can be inhibited through succinate upon accumulation by inhibition of succinate dehydrogenase (Selak et al, 2005). Interestingly, in the mouse model of lung inflammation, Tβ4 increased the levels of *Irg1* (Fig S4B), the enzyme responsible for the production of the anti-inflammatory mediator itaconate, an inhibitor of succinate dehydrogenase (Lampropoulou et al, 2016), thus raising the intriguing possibility that Tβ4, by regulating succinate levels, might modulate the levels of HIF-1α via PHDs. However, it has been reported that itaconate may also down-regulate

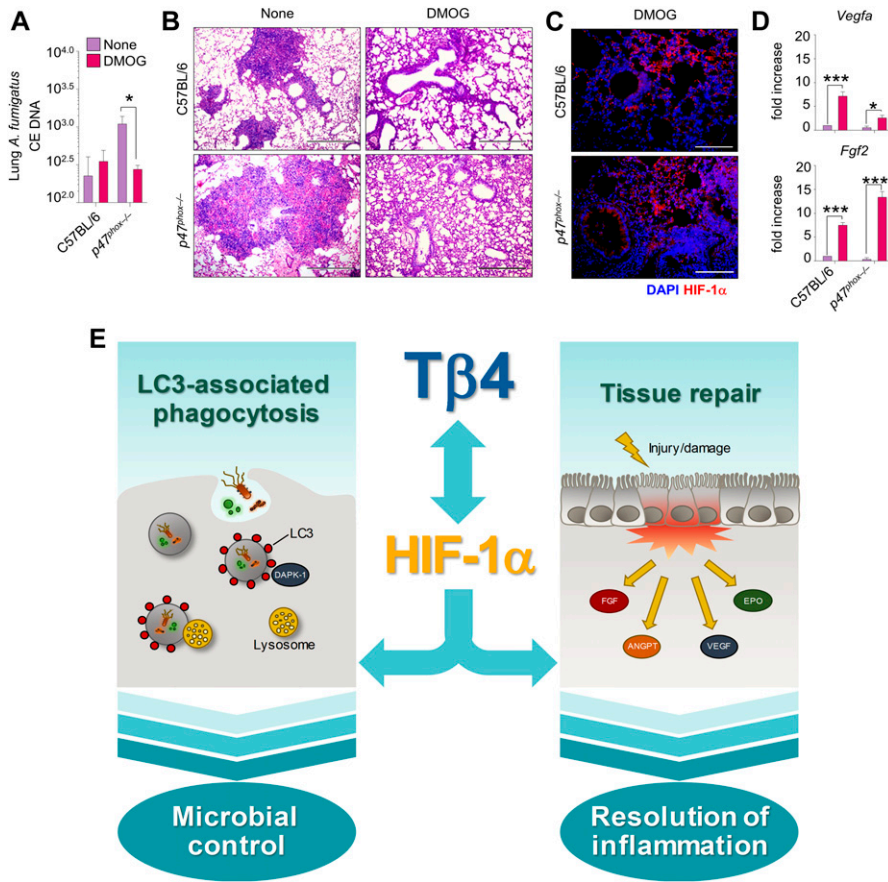


Figure 5. HIF-1 α stabilization recapitulates the effects of T β 4 in aspergillosis. C57BL/6 and p47^{phox-/-} mice were infected intranasally with *A. fumigatus* conidia and treated i.p. with 8 mg/ mouse DMOG for 5 d. (A, B, C, D) Mice were evaluated for (A) fungal growth, (B) lung histology (PAS staining), (C) HIF-1 α protein expression, and (D) *Vegfa* and *Fgf2* expression in the lung. Photographs were taken with a high-resolution microscope (Olympus BX51), 10 \times and 40 \times magnification. Gene expression was performed by RT PCR. For immunofluorescence, nuclei were counterstained with DAPI. The control group (none) for HIF-1 α immunofluorescence staining is provided in Fig 2C. For histology and immunofluorescence, data are representative of two independent experiments. For RT PCR, data are presented as mean \pm SD of at least two independent experiments. Each independent in vivo experiment includes six mice per group. * $P < 0.05$, *** $P < 0.001$, DMOG-treated versus untreated (none) mice. Two-way ANOVA, Bonferroni post hoc test. (E) The proposed model of the reciprocal regulation between T β 4 and HIF-1 α in promoting microbial control through LC3-associated phagocytosis and resolution of inflammation in CGD.

HIF-1 α levels (Lampropoulou et al, 2016). Alternatively, T β 4 might stabilize HIF-1 α through the production of mitochondrial reactive oxygen species (mtROS), as previously reported (Oh & Moon, 2010). Indeed, we could detect production of mtROS from isolated alveolar macrophages challenged with conidia and treated with T β 4 (Fig S4C and D), thus supporting the hypothesis that mtROS might mediate the regulation of HIF-1 α levels by T β 4. The ability of T β 4 to induce mtROS is reminiscent of the activity of pioglitazone, a peroxisome proliferator-activated receptor γ (PPAR γ) agonist, currently approved for the treatment of diabetes mellitus type 2 and recently proposed as a therapeutic molecule for CGD (Migliavacca et al, 2016). In normal phagocytes, PPAR γ activation linked NADPH oxidase activity with enhanced mtROS production (Fernandez-Boyanapalli et al, 2010), but this mechanism was defective in CGD. Peroxisome proliferator-activated receptor γ agonists, such as pioglitazone, could bypass the need for the NADPH oxidase for enhanced mtROS production and partially restored host defense in CGD. Given that pioglitazone is currently in a phase1/phase2 trial in CGD patients with severe infection (<https://clinicaltrials.gov/ct2/show/NCT03080480>), it will be intriguing to assess whether endogenous T β 4 is involved in the clinical efficacy of pioglitazone.

Whatever the mechanism by which T β 4 regulates HIF-1 α expression, the recent finding that HIF-1 α reprograms ILC3 metabolism for mucosal barrier protection (Di Luccia et al, 2019), offers a further plausible explanation for the protective function of T β 4 at the mucosal level.

In conclusion, by unraveling the biological activity of T β 4 in CGD, this study points to the relevance of mtROS production and HIF-1 α stabilization as druggable pathways promoting autophagy and repair in CGD.

Materials and Methods

Ethics statement

Patients and healthy volunteers gave written consent to participate as approved by the pediatric hospital Bambino Gesù Institutional Review Board. Murine experiments were performed according to the Italian Approved Animal Welfare Authorization 360/2015-PR and Legislative degree 26/2014 regarding the animal license obtained by the Italian Ministry of Health lasting for 5 yr (2015–2020).

Cell culture and treatments

RAW264.7 cells (American Type Culture Collection) were grown in supplemented Roswell Park Memorial Institute (RPMI) medium as described (De Luca et al, 2012). Cells were exposed to 10 or 100 nM of T β 4 (RegeneRx Biopharmaceuticals) for 2 and 4 h at 37 $^{\circ}$ C in 5% CO $_2$ or pretreated for 1 h with T β 4 at the same concentration before 2 h pulsing with live *A. fumigatus* conidia or inert beads (LB30; Sigma-Aldrich).

Alveolar macrophages from the lung of C57BL/6 and $p47^{phox-/-}$ uninfected mice were obtained after 2 h of plastic adherence at 37°C. Cells were treated as above and evaluated for cellular autophagy markers. Monocytes were isolated from PBMC of healthy donors or two CGD patients, harbouring the mutations c.736C>T, p.Q246X, and whole CYBB gene deletion (69, 84 kb), after informed consent, as described (De Luca et al, 2012). Cells were assessed for LC3 and HIF-1 α expression by immunofluorescence.

Mice

The 6- to 8-wk C57BL/6 (wild type, WT) mice were purchased from Charles River (Calco). Genetically engineered homozygous $p47^{phox-/-}$ mice were bred at the Animal Facility of Perugia University, Perugia, Italy.

Fungal infection and treatments

Viable conidia from the *A. fumigatus* Af293 strain were obtained as described (De Luca et al, 2012). Mice were anesthetized in a plastic cage by inhalation of 3% isoflurane (Forane Abbott) in oxygen before intranasal instillation of 2×10^7 resting conidia/20 μ l saline. For survival curves, $p47^{phox-/-}$ mice were challenged with 3×10^9 conidia/20 μ l saline. Thymosin β 4 was administered i.p. at a dose of 5 mg/kg as an effective dose as described (Badamchian et al, 2003), every day in concomitance with (days 0 \rightarrow 7) or after (days 7 \rightarrow 14) infection. Dimethylolalylglycine (Merck Millipore) was administered i.p. at a dose of 8 mg/mouse concomitantly to the infection. For *Hif1a* (duplex name mm.Ri.Hif1a.13.1; 5'-GAUAUGUUUACUAAAGGACAAGUCA-3'; 3'-UACUAUACAAUGAUUUUCCUGUUCAGU-5') and *Tmsb4x* silencing (duplex name mm.Ri.Tmsb4x.13.1; 5'-CACAUCAAAGAAUCAGAACUACUGA-3'; 3'-AAGUGUAGUUUCUUGAGUCUUGAUGACU-5'), each mouse received intranasal administration of 10 mg/kg unmodified siRNA or equivalent dose of nonspecific control siRNA duplex in a volume of 20 μ l of duplex buffer (IDT). Intranasal siRNA was given once the day before infection and 1, 3, and 5 d after infection (Iannitti et al, 2013b). It is known that lung-specific siRNA delivery can be achieved by intranasal administration without the use of viral vectors or transfection agents in vivo (Iannitti et al, 2013a). Mice were euthanized 7 or 14 d post-infection. Fungal burden was determined by quantitative PCR and expressed as conidial equivalents. Lung tissue was aseptically removed and homogenized in 3 ml of sterile saline. Lung homogenates were subjected to a secondary homogenization step with 0.5 mm glass beads in Bead Beater homogenizer (Gemini BV) and then processed for DNA extraction with the QIAamp DNA Mini Kit (QIAGEN) according to the manufacturer's directions. Fungal burden was quantified by quantitative PCR by using the sequences for the multicopy 18S ribosomal DNA gene. For lung histology, sections (3–4 μ m) of paraffin-embedded tissues were stained with periodic acid-Schiff.

DSS-induced colitis

DSS (2.5% wt/vol, 36,000–50,000 kD; MP Biomedicals) was administered in drinking water ad libitum for 7 d. Fresh solution was replaced on day 3. Mice were injected with 5 mg/kg of T β 4 every day i.p. in concomitance with (days 0 \rightarrow 7) or after (days 7 \rightarrow 14) DSS administration. The control received the diluent alone. Weight loss,

stool consistency, and faecal blood were recorded daily. Upon necropsy (7 and 14 d after DSS administration), tissues were collected for histology and cytokine analysis. Colonic sections were stained with hematoxylin and eosin. The colitis disease activity index was calculated daily for each mouse based on weight loss, occult blood, and stool consistency. A score of 1–4 was given for each parameter as described (McNamee et al, 2011).

Immunoblotting

For immunoblotting, organs or cells were lysed in Radio-Immuno-precipitation Assay buffer. The lysate was separated in SDS-PAGE and transferred to a nitrocellulose membrane. The membranes were incubated with the following primary antibodies at 4°C overnight: anti-DAPK1 (antibodies-online.com), anti-Rubicon and anti-NLRP3 (Cell Signaling), anti-T β 4 (Abcam), and anti-LC3B (Novus; Cell Signaling or Abcam). Normalization was performed by probing the membranes with mouse anti- β -actin and anti-Gapdh antibodies (Sigma-Aldrich). Normalization was performed on mouse β -actin or Gapdh, and corresponding pixel density was depicted. LC3-II band density was normalized to LC3-I to obtain the ratio. The ratio of the untreated control was set as one. Chemiluminescence detection was performed with LiteAblot Plus chemiluminescence substrate (EuroClone S.p.A.), using the ChemiDoc™ XRS+ Imaging System (Bio-Rad) and quantification was obtained by densitometry image analysis using Image Lab 5.1 software (Bio-Rad).

Immunofluorescence staining

For immunofluorescence, monocytes from CGD patients or controls were grown in supplemented RPMI and placed on microscope glass slides at 37°C for adhesion. Slides were then washed with PBS and fixed with 4% of paraformaldehyde. Cells were incubated in blocking solution (PBS-3% BSA-0.1% Triton X-100) with anti-LC3B antibody (Nanotools) and anti-HIF-1 α (Abcam). After overnight staining with primary antibodies, slides were washed and incubated with anti-IgG and rabbit-TRITC (Sigma-Aldrich). Alexa Fluor 488 phalloidin was used for selective labelling of F-actin. LC3B (Abcam), T β 4 (Abclonal), HIF-1 α , and NLRP3 (Abcam) staining of lung sections were performed as described. Nuclei were counterstained with DAPI. Images were acquired using a fluorescence microscope (BX51; Olympus) and analysis image processing software (Olympus).

RT PCR

Real-time PCR was performed using CFX96 Touch RT PCR Detection System and SYBR Green chemistry (Bio-Rad). Organs or cells from pooled mice (n = 6–8 mice/group for lungs and n = 10 mice/group for colons) were lysed, and total RNA was reverse transcribed with PrimeScript RT Reagent Kit with gDNA Eraser (Takara), according to the manufacturer's instructions. The PCR primers sequences (5'-3') are as follows:

Ptmb4: ACAAAACCCGATATGGCTGAG and GCCAGCTTGCTTCTTGT
Hif1a: TCAAGTCAGCAACGTGGAAG and TTCACAAATCAGCACCAAGC
Hif1b: CAAGCATCTTCTCACTGATC and ACACCACCCGTCCAGTCTCA
Cldn1: AGCCAGGAGCCTCGCCCCGAGCTGCA and CGGGTTGCTGCAAAGT

Ocln: GTTGATCCCCAGGAGGCTAT and CCATCTTTCTTCGGGTTTTTC
Vegfa: CAGGCTGCTGTAACGATGAA and GCATTACATCTGCTGTGCT
Fgf2: CGACCCACACGTCAACTAC and GCCGTCCATCTTCCTTCATA
Bnip3: GCTCCCAGACACCACAAGAT and TGAGAGTAGCTGTGCGCTTC
Bnip3l: CCTCGTCTCCATCCACAAT and GTCCTGCTGGTATGCATCT
Angpt2: GAACCAGACAGCAGCACAAA and TGGTCTGATCCAAAATCTGCT
Tie2: CGGCCAGGTACATAGGAGGAA and TCACATCTCCGAACAATCAGC
Epo: ACTCTCCTTGCTACTGATTCT and ATCGTGACATTTTCTGCTCC
Cxcr4: GGGTCATCAAGCAAGGATGT and GGCAGAGCTTTTGAACCTGG
Dapk1: CCTGGGTCTTGAGGCAGATA and TCGCTAATGTTTCTTGCTGG
Ldha: AGGCTCCCCAGAACAAGATT and TCTCGCCCTTGAGTTTGTCT
Pkm: CGATCTGTGGAGATGCTGAA and AATGGGATCAGATGCAAAGC
Glut1: GCTGTGCTTATGGGCTTCTC and CACATACATGGGCACAAAAGC
Irg1: AGTCCAACACCTCCAGCAC and GGTGCCATGTGTCATCAAAA

Amplification efficiencies were validated and normalized against *Gapdh*. The thermal profile for SYBR Green RT PCR was at 95°C for 3 min, followed by 40 cycles of denaturation for 30 s at 95°C, and an annealing/extension step of 30 s at 60°C. Each data point was examined for integrity by analysis of the amplification plot.

ELISA

To evaluate cytokine production in DSS-induced colitis, colons were opened longitudinally and washed in complete medium with antibiotics and were cultured at 37°C for 24 h in RPMI and 5% FBS. The supernatants were collected for ELISA. The levels of cytokines were determined by using specific ELISAs (R&D Systems) in accordance with the manufacturer's protocols. The concentration of secreted cytokines in the colon supernatants or lung homogenates was normalized to total tissue protein by using Quant-iT Protein Assay Kit (Life Technologies). Results are expressed as picogram of cytokine per microgram of total protein. The myeloperoxidase (MPO) content in colonic tissues were determined using commercially available kits (Nanjing Jiancheng Bioengineering Institute).

Antifungal effector activity

Murine polymorphonuclear (PMN) cells from C57BL/6 or *p47^{phox}-/-* uninfected mice were positively selected with magnetic beads (Miltenyi Biotec) from the peritoneal cavity of mice 8 h after the intraperitoneal injection of 1 ml endotoxin-free 10% thioglycolate solution. On FACS analysis, Gr-1⁺PMNs were 98% pure and stained positive for the CD11b myeloid marker. Monolayers of plastic-adherent macrophages were obtained, after 2 h plastic adherence, from the lung of C57BL/6 and *p47^{phox}-/-* uninfected mice. Cells were pretreated for 1 h with different concentrations of Tβ4 (10 and 100 nM) before pulsing with *A. fumigatus* conidia (1:3 cell:fungus for phagocytosis and 10:1 cell:fungus for conidiocidal activity) for 120 min at 37°C. The percentage of CFU inhibition (mean ± SD) was determined as described previously (Bellocchio et al, 2004).

ROS determination

Alveolar macrophages from the lung of C57BL/6 and *p47^{phox}-/-* uninfected mice were assessed for intracellular ROS production by dihydrorhodamine 123 (DHR) evaluation. As an inhibitor, we used

MitoTEMPO to scavenge mitochondrial ROS. For ROS determination, 10 μM DHR (Sigma-Aldrich) was added to cells exposed to 100 nM Tβ4, 10 ng/ml PMA (phorbol 12-myristate 13-acetate) (Sigma-Aldrich), and/or *A. fumigatus* conidia at cell:fungus of 1:1 for 1 h at 37°C. Cells were plated on a 96-well culture plate in HBSS buffer with Ca²⁺ and Mg²⁺ but without phenol red. Cells were preincubated with 50 μM MitoTEMPO (Enzo Life Science) for 1 h before the addition of Tβ4. The DHR was measured by the multifunctional microplate reader Tecan Infinite 200 (Tecan) at different time points. The results expressed as relative fluorescence units are the means ± SD of at least two experiments in duplicate.

Statistical analysis

GraphPad Prism 6.01 program (GraphPad Software) was used for analysis. Data are expressed as mean ± SD. Statistical significance was calculated by using two-way ANOVA (Tukey or Bonferroni post hoc test) for multiple comparisons and unpaired *t* test for single comparisons. Statistical analysis of the survival curves was performed using the log-rank (Mantel-Cox) test. The variance was similar in the groups being compared. Cell fluorescence intensity was measured by using ImageJ software.

Supplementary Information

Supplementary Information is available at <https://doi.org/10.26508/lsa.201900432>.

Acknowledgements

This study was supported by the Specific Targeted Research Project FunMeta (ERC-2011-AdG-293714 to L.Romani). MM Bellet was supported by a fellowship from Fondazione Umberto Veronesi.

Author Contributions

G Renga: conceptualization, data curation, supervision, investigation, and methodology.
V Oikonomou: conceptualization, data curation, supervision, investigation, and methodology.
S Moretti: conceptualization and data curation.
C Stincardini: investigation and methodology.
MM Bellet: supervision and writing—original draft.
M Pariano: investigation and methodology.
A Bartoli: supervision and writing—original draft.
S Brancorsini: investigation and methodology.
P Mosci: investigation and methodology.
A Finocchi: resources.
P Rossi: resources.
C Costantini: supervision and writing—original draft, review, and editing.
E Garaci: supervision and writing—original draft.
AL Goldstein: supervision and writing—original draft.

L Romani: conceptualization, supervision, funding acquisition, project administration, and writing—original draft, review, and editing.

Conflict of Interest Statement

One of the authors AL Goldstein is chairman of the board and a holder of stock in RegeneRX Biopharmaceuticals, Inc., a company developing Tβ4 for the clinic. The other authors declare no competing financial interests.

References

- Aguilera MO, Beron W, Colombo MI (2012) The actin cytoskeleton participates in the early events of autophagosome formation upon starvation induced autophagy. *Autophagy* 8: 1590–1603. doi:[10.4161/autophagy.21459](https://doi.org/10.4161/autophagy.21459)
- Badamchian M, Fagarasan MO, Danner RL, Suffredini AF, Damavandy H, Goldstein AL (2003) Thymosin beta(4) reduces lethality and down-regulates inflammatory mediators in endotoxin-induced septic shock. *Int Immunopharmacol* 3: 1225–33. doi:[10.1016/S1567-5769\(03\)00024-9](https://doi.org/10.1016/S1567-5769(03)00024-9)
- Ballweber E, Hannappel E, Huff T, Stephan H, Haener M, Taschner N, Stoffler D, Aebi U, Mannherz HG (2002) Polymerisation of chemically cross-linked actin:thymosin beta(4) complex to filamentous actin: Alteration in helical parameters and visualisation of thymosin beta(4) binding on F-actin. *J Mol Biol* 315: 613–625. doi:[10.1006/jmbi.2001.5281](https://doi.org/10.1006/jmbi.2001.5281)
- Bellocchio S, Moretti S, Perruccio K, Fallarino F, Bozza S, Montagnoli C, Mosci P, Lipford GB, Pitzurra L, Romani L (2004) TLRs govern neutrophil activity in aspergillosis. *J Immunol* 173: 7406–7415. doi:[10.4049/jimmunol.173.12.7406](https://doi.org/10.4049/jimmunol.173.12.7406)
- Bellot G, Garcia-Medina R, Gounon P, Chiche J, Roux D, Pouyssegur J, Mazure NM (2009) Hypoxia-induced autophagy is mediated through hypoxia-inducible factor induction of BNIP3 and BNIP3L via their BH3 domains. *Mol Cell Biol* 29: 2570–2581. doi:[10.1128/mcb.00166-09](https://doi.org/10.1128/mcb.00166-09)
- Bialik S, Kimchi A (2006) The death-associated protein kinases: Structure, function, and beyond. *Annu Rev Biochem* 75: 189–210. doi:[10.1146/annurev.biochem.75.103004.142615](https://doi.org/10.1146/annurev.biochem.75.103004.142615)
- Campbell EL, Bruyninckx WJ, Kelly CJ, Glover LE, McNamee EN, Bowers BE, Bayless AJ, Scully M, Saeedi BJ, Golden-Mason L, et al (2014) Transmigrating neutrophils shape the mucosal microenvironment through localized oxygen depletion to influence resolution of inflammation. *Immunity* 40: 66–77. doi:[10.1016/j.immuni.2013.11.020](https://doi.org/10.1016/j.immuni.2013.11.020)
- Campbell EL, Colgan SP (2019) Control and dysregulation of redox signalling in the gastrointestinal tract. *Nat Rev Gastroenterol Hepatol* 16: 106–120. doi:[10.1038/s41575-018-0079-5](https://doi.org/10.1038/s41575-018-0079-5)
- Colgan SP, Curtis VF, Lanis JM, Glover LE (2015) Metabolic regulation of intestinal epithelial barrier during inflammation. *Tissue Barriers* 3: e970936. doi:[10.4161/21688362.2014.970936](https://doi.org/10.4161/21688362.2014.970936)
- De Luca A, Iannitti RG, Bozza S, Beau R, Casagrande A, D'Angelo C, Moretti S, Cunha C, Giovannini G, Massi-Benedetti C, et al (2012) CD4(+) T cell vaccination overcomes defective cross-presentation of fungal antigens in a mouse model of chronic granulomatous disease. *J Clin Invest* 122: 1816–1831. doi:[10.1172/jci60862](https://doi.org/10.1172/jci60862)
- de Luca A, Smeekens SP, Casagrande A, Iannitti R, Conway KL, Gresnigt MS, Begun J, Plantinga TS, Joosten LA, van der Meer JW, et al (2014) IL-1 receptor blockade restores autophagy and reduces inflammation in chronic granulomatous disease in mice and in humans. *Proc Natl Acad Sci U S A* 111: 3526–3531. doi:[10.1073/pnas.1322831111](https://doi.org/10.1073/pnas.1322831111)
- Di Luccia B, Gilfillan S, Cella M, Colonna M, Huang SC (2019) ILC3s integrate glycolysis and mitochondrial production of reactive oxygen species to fulfill activation demands. *J Exp Med* 216: 2231–2241. doi:[10.1084/jem.20180549](https://doi.org/10.1084/jem.20180549)
- Falcone EL, Abusleme L, Swamydas M, Lionakis MS, Ding L, Hsu AP, Zelazny AM, Moutsopoulos NM, Kuhns DB, Deming C, et al (2016) Colitis susceptibility in p47(phox^{-/-}) mice is mediated by the microbiome. *Microbiome* 4: 13. doi:[10.1186/s40168-016-0159-0](https://doi.org/10.1186/s40168-016-0159-0)
- Fernandez-Boyanapalli R, Frasch SC, Riches DW, Vandivier RW, Henson PM, Bratton DL (2010) PPARγ activation normalizes resolution of acute sterile inflammation in murine chronic granulomatous disease. *Blood* 116: 4512–4522. doi:[10.1182/blood-2010-02-272005](https://doi.org/10.1182/blood-2010-02-272005)
- Gemoll T, Strohkamp S, Schillo K, Thorns C, Habermann JK (2015) MALDI-imaging reveals thymosin beta-4 as an independent prognostic marker for colorectal cancer. *Oncotarget* 6: 43869–43880. doi:[10.18632/oncotarget.6103](https://doi.org/10.18632/oncotarget.6103)
- Giaccia A, Siim BG, Johnson RS (2003) HIF-1 as a target for drug development. *Nat Rev Drug Discov* 2: 803–811. doi:[10.1038/nrd1199](https://doi.org/10.1038/nrd1199)
- Goldstein AL, Hannappel E, Kleinman HK (2005) Thymosin beta4: Actin-sequestering protein moonlights to repair injured tissues. *Trends Mol Med* 11: 421–429. doi:[10.1016/j.molmed.2005.07.004](https://doi.org/10.1016/j.molmed.2005.07.004)
- Goldstein AL, Hannappel E, Sosne G, Kleinman HK (2012) Thymosin beta4: A multi-functional regenerative peptide. Basic properties and clinical applications. *Expert Opin Biol Ther* 12: 37–51. doi:[10.1517/14712598.2012.634793](https://doi.org/10.1517/14712598.2012.634793)
- Grahl N, Puttikamonkul S, Macdonald JM, Gamcsik MP, Ngo LY, Hohl TM, Cramer RA (2011) In vivo hypoxia and a fungal alcohol dehydrogenase influence the pathogenesis of invasive pulmonary aspergillosis. *PLoS Pathog* 7: e1002145. doi:[10.1371/journal.ppat.1002145](https://doi.org/10.1371/journal.ppat.1002145)
- Gunzel D, Yu AS (2013) Claudins and the modulation of tight junction permeability. *Physiol Rev* 93: 525–569. doi:[10.1152/physrev.00019.2012](https://doi.org/10.1152/physrev.00019.2012)
- Henault J, Martinez J, Riggs JM, Tian J, Mehta P, Clarke L, Sasai M, Latz E, Brinkmann MM, Iwasaki A, et al (2012) Noncanonical autophagy is required for type I interferon secretion in response to DNA-immune complexes. *Immunity* 37: 986–997. doi:[10.1016/j.immuni.2012.09.014](https://doi.org/10.1016/j.immuni.2012.09.014)
- Iannitti RG, Carvalho A, Cunha C, De Luca A, Giovannini G, Casagrande A, Zelante T, Vacca C, Fallarino F, Puccetti P, et al (2013a) Th17/Treg imbalance in murine cystic fibrosis is linked to indoleamine 2,3-dioxygenase deficiency but corrected by kynurenines. *Am J Respir Crit Care Med* 187: 609–620. doi:[10.1164/rccm.201207-1346oc](https://doi.org/10.1164/rccm.201207-1346oc)
- Iannitti RG, Casagrande A, De Luca A, Cunha C, Sorci G, Ruzzi F, Borghi M, Galosi C, Massi-Benedetti C, Oury TD, et al (2013b) Hypoxia promotes danger-mediated inflammation via receptor for advanced glycation end products in cystic fibrosis. *Am J Respir Crit Care Med* 188: 1338–1350. doi:[10.1164/rccm.201305-0986oc](https://doi.org/10.1164/rccm.201305-0986oc)
- Iannitti RG, Napolioni V, Oikonomou V, De Luca A, Galosi C, Pariano M, Massi-Benedetti C, Borghi M, Puccetti M, Lucidi V, et al (2016) IL-1 receptor antagonist ameliorates inflammasome-dependent inflammation in murine and human cystic fibrosis. *Nat Commun* 7: 10791. doi:[10.1038/ncomms10791](https://doi.org/10.1038/ncomms10791)
- Jo JO, Kim SR, Bae MK, Kang YJ, Ock MS, Kleinman HK, Cha HJ (2010) Thymosin beta4 induces the expression of vascular endothelial growth factor (VEGF) in a hypoxia-inducible factor (HIF)-1α-dependent manner. *Biochim Biophys Acta* 1803: 1244–1251. doi:[10.1016/j.bbamer.2010.07.005](https://doi.org/10.1016/j.bbamer.2010.07.005)
- Kang YJ, Jo JO, Ock MS, Yoo YB, Chun BK, Oak CH, Cha HJ (2014) Over-expression of thymosin beta4 in granulomatous lung tissue with active pulmonary tuberculosis. *Tuberculosis (Edinb)* 94: 323–331. doi:[10.1016/j.tube.2014.01.003](https://doi.org/10.1016/j.tube.2014.01.003)
- Kumar S, Gupta S (2011) Thymosin beta 4 prevents oxidative stress by targeting antioxidant and anti-apoptotic genes in cardiac fibroblasts. *PLoS One* 6: e26912. doi:[10.1371/annotation/af7b47d5-5246-4e90-9691-f5894e119c60](https://doi.org/10.1371/annotation/af7b47d5-5246-4e90-9691-f5894e119c60)
- Kyoko OO, Kono H, Ishimaru K, Miyake K, Kubota T, Ogawa H, Okumura K, Shibata S, Nakao A (2014) Expressions of tight junction proteins Occludin and Claudin-1 are under the circadian control in the mouse large intestine: Implications in intestinal permeability and

- susceptibility to colitis. *PLoS One* 9: e98016. doi:[10.1371/journal.pone.0098016](https://doi.org/10.1371/journal.pone.0098016)
- Lampropoulou V, Sergushichev A, Bambouskova M, Nair S, Vincent EE, Loginicheva E, Cervantes-Barragan L, Ma X, Huang SC, Griss T, et al (2016) Itaconate links inhibition of succinate dehydrogenase with macrophage metabolic remodeling and regulation of inflammation. *Cell Metab* 24: 158–166. doi:[10.1016/j.cmet.2016.06.004](https://doi.org/10.1016/j.cmet.2016.06.004)
- Lassen KG, Xavier RJ (2018) Mechanisms and function of autophagy in intestinal disease. *Autophagy* 14: 216–220. doi:[10.1080/15548627.2017.1389358](https://doi.org/10.1080/15548627.2017.1389358)
- Limper AH, Colby TV, Sanders MS, Asakura S, Roche PC, DeRemee RA (1994) Immunohistochemical localization of transforming growth factor-beta 1 in the nonnecrotizing granulomas of pulmonary sarcoidosis. *Am J Respir Crit Care Med* 149: 197–204. doi:[10.1164/ajrccm.149.1.8111583](https://doi.org/10.1164/ajrccm.149.1.8111583)
- Martinez J, Cunha LD, Park S, Yang M, Lu Q, Orchard R, Li QZ, Yan M, Janke L, Guy C, et al (2016) Noncanonical autophagy inhibits the autoinflammatory, lupus-like response to dying cells. *Nature* 533: 115–119. doi:[10.1038/nature17950](https://doi.org/10.1038/nature17950)
- McNamee EN, Masterson JC, Jedlicka P, McManus M, Grenz A, Collins CB, Nold MF, Nold-Petry C, Bufler P, Dinarello CA, et al (2011) Interleukin 37 expression protects mice from colitis. *Proc Natl Acad Sci U S A* 108: 16711–16716. doi:[10.1073/pnas.1111982108](https://doi.org/10.1073/pnas.1111982108)
- Migliavacca M, Assanelli A, Ferrua F, Cicalese MP, Biffi A, Frittoli M, Silvani P, Chidini G, Calderini E, Mandelli A, et al (2016) Pioglitazone as a novel therapeutic approach in chronic granulomatous disease. *J Allergy Clin Immunol* 137: 1913–1915 e1912. doi:[10.1016/j.jaci.2016.01.033](https://doi.org/10.1016/j.jaci.2016.01.033)
- Mole DR, Schlemminger I, McNeill LA, Hewitson KS, Pugh CW, Ratcliffe PJ, Schofield CJ (2003) 2-oxoglutarate analogue inhibitors of HIF prolyl hydroxylase. *Bioorg Med Chem Lett* 13: 2677–2680. doi:[10.1016/s0960-894x\(03\)00539-0](https://doi.org/10.1016/s0960-894x(03)00539-0)
- Oh JM, Moon EY (2010) Actin-sequestering protein, thymosin beta-4, induces paclitaxel resistance through ROS/HIF-1alpha stabilization in HeLa human cervical tumor cells. *Life Sci* 87: 286–293. doi:[10.1016/j.lfs.2010.07.002](https://doi.org/10.1016/j.lfs.2010.07.002)
- Oh JM, Ryou IJ, Yang Y, Kim HS, Yang KH, Moon EY (2008) Hypoxia-inducible transcription factor (HIF)-1 alpha stabilization by actin-sequestering protein, thymosin beta-4 (TB4) in HeLa cervical tumor cells. *Cancer Lett* 264: 29–35. doi:[10.1016/j.canlet.2008.01.004](https://doi.org/10.1016/j.canlet.2008.01.004)
- Oikonomou V, Moretti S, Renga G, Galosi C, Borghi M, Pariano M, Puccetti M, Palmerini CA, Amico L, Carotti A, et al (2016) Noncanonical fungal autophagy inhibits inflammation in response to IFN-gamma via DAPK1. *Cell Host Microbe* 20: 744–757. doi:[10.1016/j.chom.2016.10.012](https://doi.org/10.1016/j.chom.2016.10.012)
- Oikonomou V, Renga G, De Luca A, Borghi M, Pariano M, Puccetti M, Paolicelli G, Stincardini C, Costantini C, Bartoli A, et al (2018) Autophagy and LAP in the fight against fungal infections: Regulation and therapeutics. *Mediators Inflamm* 2018: 6195958. doi:[10.1155/2018/6195958](https://doi.org/10.1155/2018/6195958)
- Palazon A, Goldrath AW, Nizet V, Johnson RS (2014) HIF transcription factors, inflammation, and immunity. *Immunity* 41: 518–528. doi:[10.1016/j.immuni.2014.09.008](https://doi.org/10.1016/j.immuni.2014.09.008)
- Petersen HJ, Smith AM (2013) The role of the innate immune system in granulomatous disorders. *Front Immunol* 4: 120. doi:[10.3389/fimmu.2013.00120](https://doi.org/10.3389/fimmu.2013.00120)
- Rider NL, Jameson MB, Creech CB (2018) Chronic granulomatous disease: Epidemiology, pathophysiology, and genetic basis of disease. *J Pediatric Infect Dis Soc* 7: S2–S5. doi:[10.1093/jpids/piy008](https://doi.org/10.1093/jpids/piy008)
- Romani L, Fallarino F, De Luca A, Montagnoli C, D'Angelo C, Zelante T, Vacca C, Bistoni F, Fioretti MC, Grohmann U, et al (2008) Defective tryptophan catabolism underlies inflammation in mouse chronic granulomatous disease. *Nature* 451: 211–215. doi:[10.1038/nature06471](https://doi.org/10.1038/nature06471)
- Ryu YK, Kang JH, Moon EY (2014) The actin-sequestering protein thymosin beta-4 is a novel target of hypoxia-inducible nitric oxide and HIF-1alpha regulation. *PLoS One* 9: e106532. doi:[10.1371/journal.pone.0106532](https://doi.org/10.1371/journal.pone.0106532)
- Schaible B, McClean S, Selfridge A, Broquet A, Asehounne K, Taylor CT, Schaffer K (2013) Hypoxia modulates infection of epithelial cells by *Pseudomonas aeruginosa*. *PLoS One* 8: e56491. doi:[10.1371/journal.pone.0056491](https://doi.org/10.1371/journal.pone.0056491)
- Selak MA, Armour SM, MacKenzie ED, Boulahbel H, Watson DG, Mansfield KD, Pan Y, Simon MC, Thompson CB, Gottlieb E (2005) Succinate links TCA cycle dysfunction to oncogenesis by inhibiting HIF-alpha prolyl hydroxylase. *Cancer Cell* 7: 77–85. doi:[10.1016/j.ccr.2004.11.022](https://doi.org/10.1016/j.ccr.2004.11.022)
- Shepardson KM, Jhingran A, Caffrey A, Obar JJ, Suratt BT, Berwin BL, Hohl TM, Cramer RA (2014) Myeloid derived hypoxia inducible factor 1-alpha is required for protection against pulmonary *Aspergillus fumigatus* infection. *PLoS Pathog* 10: e1004378. doi:[10.1371/journal.ppat.1004378](https://doi.org/10.1371/journal.ppat.1004378)
- Simon AK, Clarke AJ (2016) Non-canonical autophagy LAPs lupus. *Cell Death Differ* 23: 1267–1268. doi:[10.1038/cdd.2016.55](https://doi.org/10.1038/cdd.2016.55)
- Singh P, Ravanan P, Talwar P (2016) Death associated protein kinase 1 (DAPK1): A regulator of apoptosis and autophagy. *Front Mol Neurosci* 9: 46. doi:[10.3389/fnmol.2016.00046](https://doi.org/10.3389/fnmol.2016.00046)
- Sosne G, Xu L, Prach L, Mrock LK, Kleinman HK, Letterio JJ, Hazlett LD, Kurpakus-Wheaton M (2004) Thymosin beta 4 stimulates laminin-5 production independent of TGF-beta. *Exp Cell Res* 293: 175–183. doi:[10.1016/j.yexcr.2003.09.022](https://doi.org/10.1016/j.yexcr.2003.09.022)
- Sprengeler EG, Gresnigt MS, van de Veerndonk FL (2016) LC3-associated phagocytosis: A crucial mechanism for antifungal host defence against *Aspergillus fumigatus*. *Cell Microbiol* 18: 1208–1216. doi:[10.1111/cmi.12616](https://doi.org/10.1111/cmi.12616)
- Takeshima H, Ikegami D, Wakabayashi M, Niwa T, Kim YJ, Ushijima T (2012) Induction of aberrant trimethylation of histone H3 lysine 27 by inflammation in mouse colonic epithelial cells. *Carcinogenesis* 33: 2384–2390. doi:[10.1093/carcin/bgs294](https://doi.org/10.1093/carcin/bgs294)
- Taylor CT, Colgan SP (2017) Regulation of immunity and inflammation by hypoxia in immunological niches. *Nat Rev Immunol* 17: 774–785. doi:[10.1038/nri.2017.103](https://doi.org/10.1038/nri.2017.103)
- Toossi Z, Gogate P, Shiratsuchi H, Young T, Ellner JJ (1995) Enhanced production of TGF-beta by blood monocytes from patients with active tuberculosis and presence of TGF-beta in tuberculous granulomatous lung lesions. *J Immunol* 154: 465–473.
- Yee Koh M, Spivak-Kroizman TR, Powis G (2008) HIF-1 regulation: Not so easy come, easy go. *Trends Biochem Sci* 33: 526–534. doi:[10.1016/j.tibs.2008.08.002](https://doi.org/10.1016/j.tibs.2008.08.002)



License: This article is available under a Creative Commons License (Attribution 4.0 International, as described at <https://creativecommons.org/licenses/by/4.0/>).